Personalized neoantigen-based immunotherapy for advanced collecting duct carcinoma: case report

Yongyi Zeng,[1,2] Wei Zhang,[3] Zhenli Li,[1,2] Youshi Zheng,[1,2] Yingchao Wang,[1,2] Geng Chen,[1,2] Liman Qiu,[1] Kun Ke,[1] Xiaoping Su,[4] Zhixiong Cai,[1,2] Jingfeng Liu,[1,2] Xiaolong Liu [ORCID] [1,2]

Correspondence to
Dr Xiaolong Liu, Mengchao Hepatobiliary Hospital of Fujian Medical University, Fuzhou 350025, China; xiaoloong.liu@gmail.com

Professor Jingfeng Liu, Mengchao Hepatobiliary Hospital of Fujian Medical University, Fuzhou 230025, China; drjingfeng@126.com

ABSTRACT

Background Collecting duct carcinoma (CDC) of the kidney is a rare and highly aggressive malignant tumor with the worst prognosis among all renal cancers. Nevertheless, the first-line treatments, including chemotherapy and target therapy, usually show poor response to CDC. Recent studies have suggested that immunotherapy targeting personal tumor-specific neoantigens could be a promising strategy for several solid cancers. However, whether it has therapeutic potential in CDC remains unclear.

Case presentation Here, we report a case of an Asian patient who underwent personalized neoantigen-based immunotherapy. The patient was diagnosed with metastatic CDC and suffered extensive tumor progression following sorafenib treatment. Based on the patient's own somatic mutational profile, a total of 13 neoantigens were identified and corresponding long-peptide vaccine and neoantigen-reactive T cells (NRTs) were prepared. After six cycles of neoantigen-based vaccination and T-cell immunotherapy, the patient was reported with stable disease status in tumor burden and significant alleviation of bone pain. Ex vivo interferon-γ enzyme-linked immunospot assay proved the reactivity to 12 of 13 neoantigens in peripheral blood mononuclear cells collected after immunotherapy, and the preferential reactivity to mutant peptides compared with corresponding wild-type peptides was also observed for 3 of the neoantigens. Surprisingly, biopsy sample collected from CDC sites after 3 months of immunotherapy showed decreased mutant allele frequency corresponding to 92% (12/13) of the neoantigens, indicating the elimination of tumor cells carrying these neoantigens.

Conclusions Our case report demonstrated that the combined therapy of neoantigen peptide vaccination and NRT cell infusion showed certain efficacy in this CDC case, even when the patient carried only a relatively low tumor mutation burden. These results indicated that the personalized neoantigen-based immunotherapy was a promising new strategy for advanced CDC.

Trial registration number ChiCTR1800017836.

BACKGROUND

Collecting duct carcinoma (CDC), a rare malignant tumor occurring in the kidney parenchyma epithelium, originates from the collecting duct of renal medulla, accounting for less than 1% of the common renal cell cancer.[1 2] Although surgical treatment is the preferred option for CDC, most patients usually suffer from extensive metastasis with extremely poor prognosis at the time of diagnosis, and thus lost their chance of surgery.[3] Other treatments, such as chemotherapy and target therapy, also showed great potential but generally achieved poor response clinically.[4] Therefore, there is an urgent need to develop novel strategies with high efficacy for CDC.

Neoantigens are epitope peptides binding with the major histocompatibility complex (MHC) on the surface of malignant cells, which can be recognized by T cells and thus elicit strong specific antitumor immune responses.[5 6] Neoantigens usually originate from non-synonymous somatic variants in cancer cells, such as point mutations, gene fusion and RNA editing events.[7 8] Since neoantigens are specifically expressed in tumor cells rather than normal cells, they could serve as ideal immunotherapeutic targets with maximized therapeutic efficacy and minimized risk of autoimmunity. With the development of next-generation sequencing and bioinformatics, neoantigen candidates that could bind to patients' own MHC molecules with high affinity could be identified by genomic and transcriptomic profiling in tumor. Furthermore, the neoantigens could be synthesized and used for different types of immunotherapy, such as neoantigen long-peptide vaccines, dendritic cell vaccines, and neoantigen-reactive T cells (NRTs). Recently, cancer immunotherapy based on neoantigens has achieved excellent therapeutic effects in multiple solid tumors, such as melanoma, small cell lung cancer, as well as gliomas with low mutation burden.[9 10] Here, we report a patient with advanced CDC with personalized

neoantigen-based immunotherapy for the first time, who achieved stable disease status for 9 months. Neoantigen-specific immune responses and tumor clonal evolution were also evaluated before and after immunotherapy.

CASE PRESENTATION
Sample collection
The patient diagnosed with advanced CDC and multiple bone metastases at Mengchao Hepatobiliary Hospital of Fujian Medical University was enrolled in this study. The CDC biopsies were collected at preimmunotherapy time point and after three treatment cycles of the neoantigen-based immunotherapy. Corresponding blood samples were collected at the same time points. Available CT/MRI scans were also acquired. This is a single-centre, single arm clinical study of an individualized neoantigen peptide vaccine combined with NRTs in the treatment of advanced malignancies retrospectively registered in 17 August 2018 (http://www.chictr.org.cn/showproj.aspx?proj=30138).

Whole-exome DNA and RNA sequencing
Tumor tissues obtained by needle biopsy and peripheral blood samples were used for whole-exome sequencing (WES) and RNA sequencing. In brief, after DNA/RNA extraction and library construction, both enriched exome and transcriptome libraries were sequenced by Annoroad Gene Tech. (Beijing) Co. on Illumina HiSeq X10 platform (paired end, 150 bp).

Sequencing data process and epitope prediction
WES read pairs were aligned to UCSC human reference genome hg19 (GRCh37) using BWA.[11] Somatic mutations were detected with Mutect2 and Somaticsniper, and then further confirmed by DeepSNV.[12] Indels were detected by Metect2 and Strelka, and manually confirmed by Integrative Genomics Viewer at both DNA and RNA levels. For RNA-seq, the qualified reads were aligned to human genome reference (GRCh37) with GENCODE gene annotation using STAR.[13] To quantify the expression levels for each gene, transcripts per kilobase per million mapped reads (TPM) were calculated.

To keep high-quality somatic mutations for following neoantigen identification, all mutations consistently identified by Mutect2 and Somaticsniper were further filtered with following criteria: ≥20× depth in both tumor tissues and peripheral blood samples, variant reads≥5 and variant allele frequency (VAF)≥10% in tumor tissues, and VAF≥1% in blood samples. All the qualified mutations were further confirmed at RNA level by DeepSNV[14] that mutations≥20× depth and VAF≥10% in tumor tissue were kept, and the expression level of their corresponding genes should be with TPM≥1. All qualified mutations were annotated by variant effect predictor.[15] For each nonsynonymous mutation, all possible peptides containing mutated amino acids with length ranging from 8 to 11 mer were extracted, and their binding affinity to

corresponding patient's human leukocyte antigen (HLA) class I alleles (HLA-A, HLA-B and HLA-C) was predicted by NetMHCpan V.4.0. Meanwhile, the binding affinity of 15 mer peptides containing mutated amino acids to patient's HLA class II alleles (HLA-DRB1) was also evaluated using NetMHCpanII V.3.1.[16 17] Peptides with IC$_{50}$<500 nM were predicted to be candidate epitopes.

Clonal evolution assessment
Clonal evolution analysis of preimmunotherapy and postimmunotherapy tumor samples was conducted by SciClone[18] using all the qualified somatic mutations passing aforementioned criteria.

HLA genotyping
Patient four-digit HLA class I genotype was assessed by OptiType,[19] and the HLA class II alleles were assessed by Seq2HLA[20] using RNA-seq data. Additionally, the HLA typing was further confirmed by PCR sequence-based typing.

Long-peptide synthesis and the preparation of neoantigen long-peptide vaccine
The therapeutic duration is 180 days for this patient; days 0–60 were the period for neoantigen peptide vaccine preparation. Afterwards, each 30 days were assigned as one treatment cycle. Thirteen personalized neoantigen peptides (27 amino acids in length) were synthesized by the standard solid-phase synthetic peptide chemistry and purified using reverse-phase high-performance liquid chromatography (GenScript USA) with strict quality control (>98% purity, endotoxin concentration was less than 0.01 EU/g and TFA (trifluoroacetic acid) residue was less than 1%). All peptides were divided into three pools containing four to five peptides for each (designated as pools A-C, 0.3 mg/peptide) and mixed with 0.5 mg poly:IC (polyinosinic-polycytidylic acid injection, Guangdong South China Pharmaceutical. Co) as the peptide vaccines. Each pool was administered by subcutaneous injection to one of the limbs (right armpit, left axilla, right groin and left groin).

NRT cell preparation
One hundred millilitres of the patient's own blood was collected by monocyte blood collection machine, then the PBMCs were isolated and cultured in culture dish for 2 hours to further separate dentritic cells (adherent cell) and T cells (non-adherent cell). Afterwards, the adherent cells were cultured with medium (1% autologous serum+KBM581+1000 U/mL rhGM-CSF (recombinant human granulocyte-macrophage colony-stimulating factor)+500 U/mL interleukin (IL)-4) for 48 hours, and then loaded with 13 neoantigen peptides (25 μg/peptide) accompanied by certain cytokines (tumor necrosis factor alpha, 1000 U/mL; IL-1b, 10 ng/mL; IL-6, 1000 U/mL) in the medium to induce DC maturation overnight. The maturated DCs were cocultured with T cells (0.5–1×10^6 cells/mL) at a ratio of 1:10 in a culture bag containing 5% autologous plasma+KBM581+100 U/mL IL-2+20 ng/

mL IL-7 for 48 hours. Afterwards, the primary NRT cells were collected and stimulated with fresh matured DCs for another two times. The proportion of activated T cells (CD3$^+$ 4-1BB$^+$) in NRT preparation was assessed by flow cytometry. Then, the T cells were cocultured with OKT3 antibody for amplifying neoantigen-specific T cells to large numbers. On day 14, the prepared NRT cells were washed and resuspended with normal saline and administered to quality control (endotoxin testing ≤5 EU/mL, a negative result for mycoplasma and sterile detection) before cell infusion.

Interferon (IFN)-γ enzyme-linked immunospot (ELISPOT) assay

IFN-γ secretion of neoantigen-specific T cells was measured by ELISPOT using Human IFN-γ ELISpot^{plus} kit (MABTECH) according to the manufacturer's instruction. Briefly, the DC cells (2×10^4) were stimulated with neoantigen peptide pool (2 µg in total, 0.15 µg per peptide) or each synthesized neoantigen peptide (2 µg) for 24 hours at 37°C with 5% CO_2. Then, 2×10^5 PBMCs were pretreated with IL-2 (50 U/mL) for 24 hours and cocultured with the peptide-simulated DC cells (2×10^4) at 37°C for another 24 hours in a 96-well plate. The plates were washed and subsequently incubated with detection antibody (7-B6-1,1 µg/mL) for 2 hours at room temperature. The plates were washed again and then incubated with streptavidin–horseradish peroxidase (1:1000 dilution) for 1 hour at room temperature. Subsequently, TMB (3, 3′, 5, 5′-Tetramethylbenzidine) substrate solution was added to each well and incubated for 15–25 min at room temperature before adding deionized water to stop the reaction. Finally, the spots were imaged and analyzed.

RESULTS
Case report

A 73-year-old Asian patient was first admitted to Mengchao Hepatobiliary Hospital of Fujian Medical University due to tenderness pain of spinal and percussive pain of renal. Routine blood and biochemical tests showed no obvious abnormalities. MRI scan revealed a 4.2×3.7 cm nodular in the right kidney, accompanied by multiple bone metastases (L1: 1.4×1.0 cm, L2: 1.8×1.4 cm, L5: 1.5×2.0 cm). As shown in figure 1A, the kidney nodule and bone marrow biopsies were diagnosed as metastatic CDC by a pathologist using H&E examination. Then, the patient subsequently underwent vertebroplasty and sorafenib treatment (400 mg, two times per day) within 2 months. Unfortunately, the patient suffered extensive tumor progression in CDC (MRI scan: 5.7×4.2 cm) and bone metastases (L1: 2.3×2.0 cm, L2: 2.5×2.2 cm, L5: 2.3×1.3 cm).

As poor performance status of the standard first-line treatment and lack of other treatment options, the patient underwent personalized neoantigen immunotherapy based on his own tumor somatic mutation profile. To obtain his tumor-specific neoantigens, a needle biopsy collected from CDC and matched peripheral blood mononuclear cells (PBMCs) were subjected to whole exome sequencing and transcriptomic sequencing. In total, 48 qualified nonsynonymous somatic mutations and seven somatic indels were identified (online supplementary tables S1 and S2), while only 18 of these somatic mutations and 2 of these indels were confirmed at RNA level. To identify reliable neoantigens for clinical preparation of peptide vaccine and NRT cells, we only included 13 somatic mutations with VAF>10% at both DNA and RNA level. Binding affinity prediction of the mutated peptides showed that peptides generated from 12 of the 13 mutations had high affinity (IC50<150 nM) to HLA
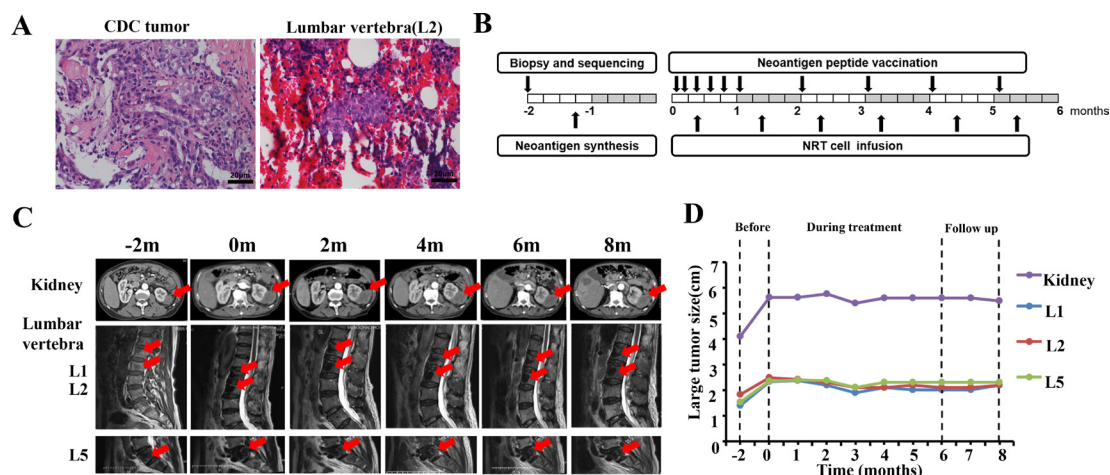

Figure 1 Diagnostic assessment, treatment, and clinical monitoring of the patient with CDC. (A) Pretreatment assessment of primary CDC tumor and bone metastasis lesion, as determined by pathological examination of H&E-stained needle biopsies. (B) Timeline presentation of the treatment dates of personalized neoantigen peptide vaccination and NRT infusion. (C,D) Timeline of kidney and lumbar vertebra CT scans and the corresponding tumor size during neoantigen-based immunotherapy. The red arrows indicate the primary tumor lesion (upper panel) and metastatic tumor lesions (lower panel). CDC, collecting duct carcinoma; NRT, neoantigen-reactive T cell.

Table 1 Personalized neoantigen peptides and predicted HLA binding in the enrolled patient

ID	Mutation	Gene	HLA	Peptide_MT	IC50(MT)
chr13_37016372	L426R	CCNA1	HLA-DRB1*12:02	SEIVPCLSERHKAYL	41.73
chr1_234519474	K50N	COA6	HLA-DRB1*12:02	QWINYFDKRRDYLKF	37.43
chr5_54558630	V1219E	DHX29	HLA-A*02:03	LLKAELVAGL	6.8
chr17_45451923	K321N	EFCAB13	HLA-DRB1*12:02	VAGCYLKYKNKNSLS	37.16
chr1_225700405	A706V	ENAH	HLA-DRB1*12:02	EMSALLARRRRIVEK	3.24
chr12_25398284	G12D	KRAS	HLA-A*02:03	KLVVVGADGV	38.1
chr19_42907156	A857E	LIPE	HLA-DRB1*12:02	ALPLSEPMRRSVSEE	536.4
chrX_149828881	I 464S	MTM1	HLA-A*02:03	FLSIILDHL	6.0
chr5_7878221	S216C	MTRR	HLA-DRB1*12:02	RTDLVKSELLHIECQ	39.99
chr7_154753273	Y738C	PAXIP1	HLA-DRB1*12:02	LKLMAYLAGAKYTGC	9.4
chr7_77256204	A403G	PTPN12	HLA-DRB1*12:02	PKPVLHMVSSEQHSG	57.32
chr1_153751670	Y704C	SLC27A3	HLA-A*02:03	FLQEVNVCGV	4.1
chr16_18826602	I 3507F	SMG1	HLA-DRB1*12:02	SFYNNLVSFASPLVT	14.01

class I or class II alleles, including refractory mutated genes such as *KRAS* G12D (table 1). Considering that IC50 of the binding affinity for LIPE A857E peptide with HLA-DRB1*12:02 was 536 nM (near the filtering cut-off value of 500 nM), all the 13 mutations were selected for synthesizing neoantigen peptides. As long peptides may be more immunogenic than short peptides, long peptides (27aa) with the mutated amino acid in the middle were synthesized for the preparation of both peptide vaccine and NRTs.

The patient underwent a total of six treatment cycles of neoantigen-based immunotherapy (figure 1B). For neoantigen peptide vaccine treatment, the vaccine was given on days 1, 5, 8, 15, and 22 of treatment cycle 1 (priming phase) and was given on day 1 of subsequent treatment cycles (boosting phase). Additionally, for the NRT infusion, a total of 5×10^9 prepared NRT cells were intravenously administered in a 60 min period on day 10 of each treatment cycle, followed by continuous intravenous injection of IL-2 at 3.0 MIU for 4 days. According to the standard image diagnosis, the patient reported stable disease status in tumor burden and significant alleviation of bone pain (cut the painkiller in half) after undergoing neoantigen immunotherapy within 3 months (figure 1C,D). With immunotherapy continuously undergoing, no obvious progression in tumor burden and no obvious side effects have been observed in this patient for another three treatment cycles. During the immunotherapy and follow-up, the patient's ECOG (Eastern Cooperative Oncology Group) performance status score was steadily maintained at level 2. Unfortunately, the patient died after 3 months of finishing neoantigen-based treatments due to complications caused by an accidental fall.

Antitumor immune response assessment

PBMCs were collected from this patient at preimmunotherapy time point, and after three treatment cycles

of neoantigen-based immunotherapy (postimmunotherapy) to evaluate the presence of the antigen-specific T cells. ELISPOT assay was performed to assess the immune response following stimulation with neoantigen pools and each neoantigen individually. As shown in figure 2A, the ELISPOT results indicated that the reactivity of PBMCs against total neoantigens were significantly increased in the postimmunotherapy time point when compared with the preimmunotherapy time point. Moreover, based on the results of each individual neoantigen, 12 of the 13 mutated peptides could significantly induce strong immune responses at postimmunotherapy time point, suggesting the generation of potent immune responses against multiple predicted epitopes for this patient (figure 2B,C and online supplementary figure S1A). For 7 of these 12 responsive neoantigens, the T cells could simultaneously respond to mutated peptides and their corresponding wild-type peptides, although the response degree to mutated peptides was higher, suggesting the high degree of cross-reactivity. For another remaining five neoantigen peptides, CCNA1 L426R, LIPE A857E and KRAS G12D showed preferentially immune reactivity to T cells (>10-fold sensitivity) comparing with their corresponding wild-type peptides; the DHX29 V1219E and PAIXP1 Y738C were considered as suspected responses due to the obvious differences between two duplicate wells. In contrary, MTM1 I464S peptide showed no obvious immune reactivity to T cells, while its wild-type peptide showed strong immune reactivity. Moreover, we also analyzed the T-cell activation proportion of NRT preparation by flow cytometry analysis by evaluating $CD3^+/4-1BB^+$ T-cell percentage. As expected, the $CD3^+/4-1BB^+$ T-cell percentage was increased from 1.92% in precultured PBMCs to 7.92% in NRT preparation (figure 2D), suggesting that the NRT cells accounted for about 6% in total infusion of this patient. Here, we only achieved modest enrichment of NRT cells, which might
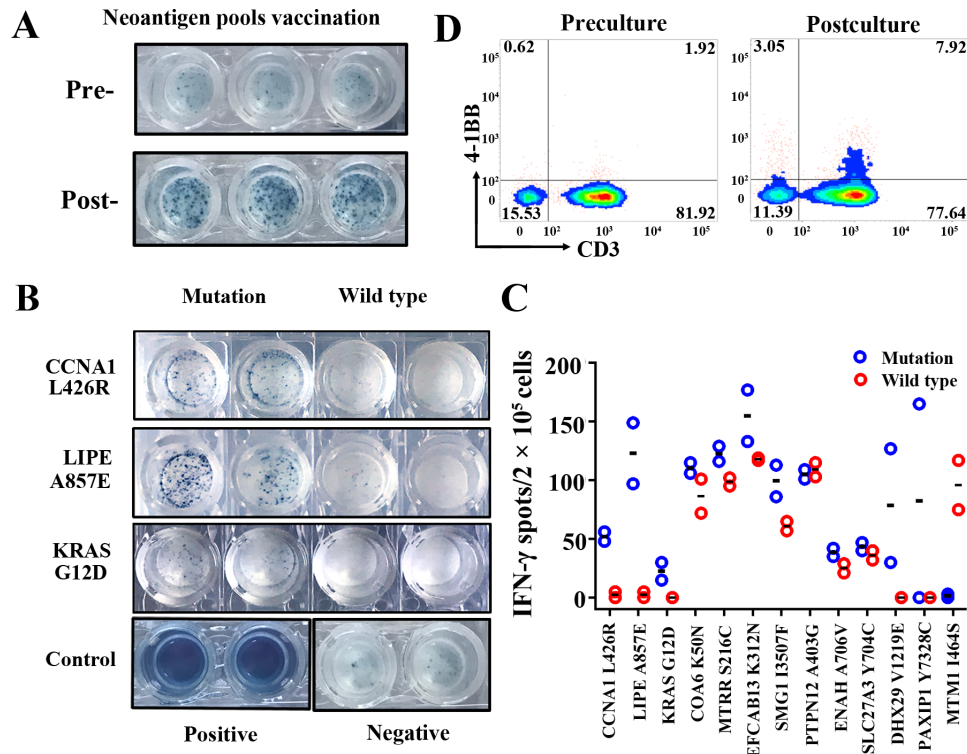
Figure 2 Monitoring of the neoantigen-induced peripheral blood T-cell responses. PBMCs collected at the time points of preimmunotherapy and postimmunotherapy were assessed for neoantigen-specific T-cell responses. (A) Comparison of IFN-γ secretion by PBMCs from preimmunotherapy and postimmunotherapy time point stimulated by neoantigen pools. (B) Images of IFN-γ secretion of PBMCs stimulated by each neoantigen (CCNA1, LIPE and KRAS) comparing with their corresponding wild-type peptides. (C) Quantitative results of IFN-γ secretion by PBMCs against autologous dendritic cells which presented 13 neoantigens individually comparing with their corresponding wild-type peptides. (D) Activated T-cell percentage (CD3+/4-1BB+ cell population) in neoantigen-reactive T-cell preparation. IFN, interferon; PBMC, peripheral blood mononuclear cell.

be associated with the enrolled patient's status, since the enrichment and activity of reactive T cells are heavily relied on the immune cell status; in our study, the patient was relatively old and underwent target drug therapy (sorafenib) before undergoing our neoantigen-based immunotherapy; these issues are well known to impair the functions of the patient's immune cells.

To investigate the effects of neoantigen-based immunotherapy on immune microenvironment, another CDC biopsy collected at postimmunotherapy time point was subjected to whole-exome sequencing and transcriptomic sequencing. First, we compared the allele frequencies of neoantigens on genomic level between biopsy from preimmunotherapy and postimmunotherapy. The result showed that the mutant allele frequency corresponding to 92% (12/13) of the neoantigens decreased (figure 3A), indicating that the immune system could indeed kill tumor cells carrying these neoantigens. Meanwhile, the mutated allele frequency of MTM1 I464S was upregulated after immunotherapy, which was well consistent with the ELISPOT examination result. However, the allele frequencies for six of eight non-targeted mutations were also decreased in the postimmunotherapy CDC biopsy, while the other two non-targeted mutations were increased (online supplementary table S3). This phenomenon might be attributed to the coexistence

of the non-targeted mutations and targeted neoantigens in tumor cells; when NRTs specifically killed tumor cells carrying such neoantigens, the frequency the non-targeted mutations possessed by the same tumor cells also decreased; additionally, the cytokines released by neoantigen-specific T cells might also have non-specific cytotoxicity on other tumor cells. Furthermore, eight new somatic mutations were identified and five of them might be new neoantigen candidates (C2CD5 V874L, IKBKB W291L, LINS L258F, TYK2 R1159C and ZDHHC20 Q339H) in the CDC biopsy after immunotherapy.

The clonal structure dynamics of CDC biopsy from preimmunotherapy and postimmunotherapy showed subtle changes in tumor clonal structure under the pressure of immunotherapy (figure 3B). Interestingly, HLA genes including MHCI (HLA-A, HLA-B and HLA-C) and MHCII (HLA-DRB1), HLA subtypes encoded by which have potential binding affinity to identified neoantigens were all upregulated in CDC biopsy after immunotherapy (online supplementary table S4 and S5). Contrarily, the expression of other HLA subtypes was mostly downregulated in CDC biopsy after immunotherapy. These results suggested that the neoantigen-based immunotherapy might promote the antigen presentation process and immune infiltration for upregulating corresponding HLA subtypes that could potentially bind with neoantigens.
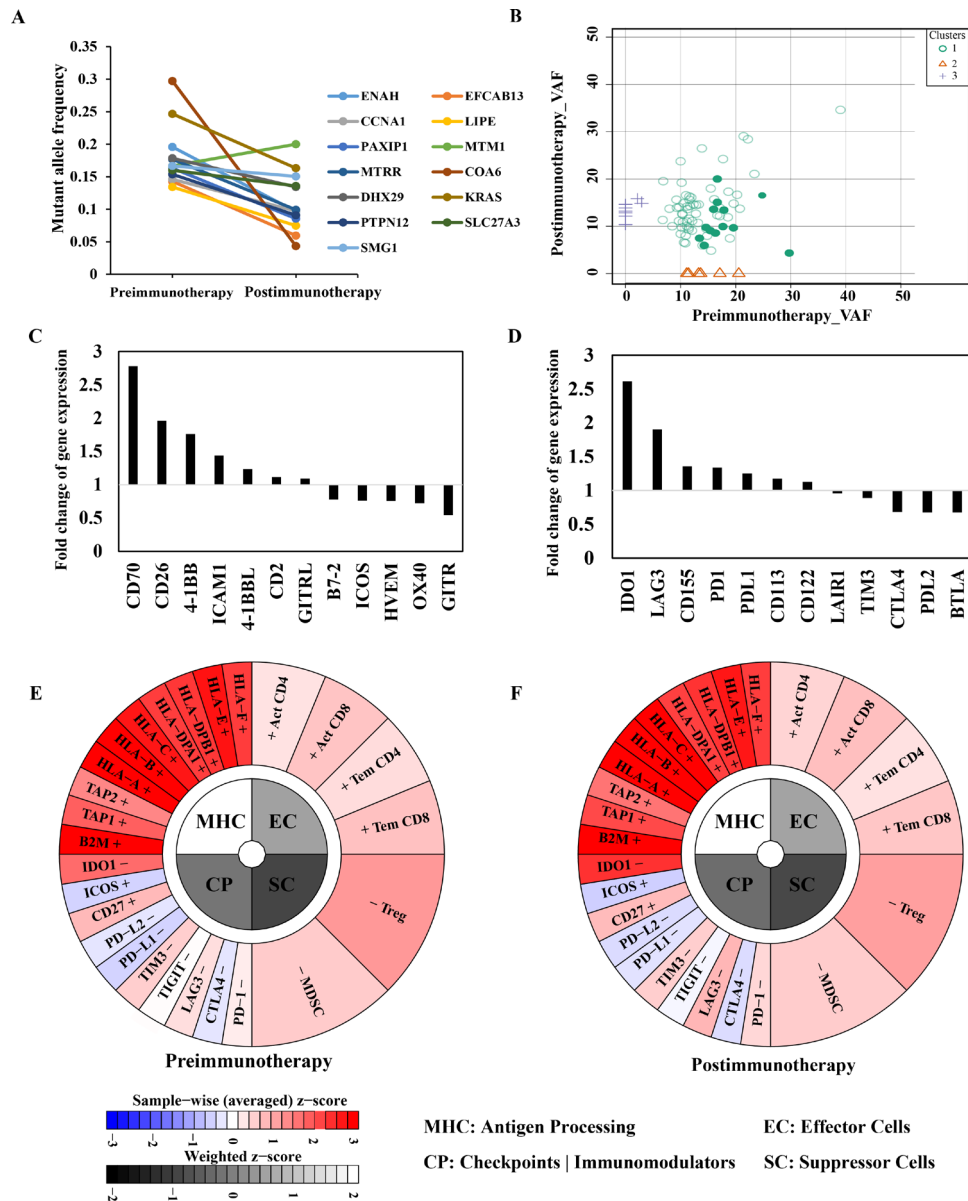
Figure 3 Immune signatures in CDC biopsies collected at preimmunotherapy and postimmunotherapy time point. (A) Mutated allele frequency of the 13 neoantigens in CDC tissues collected preimmunotherapy and postimmunotherapy. (B) Clonal evolution of tumor tissues collected preimmunotherapy and postimmunotherapy. Neoantigens were indicated by solid circles. (C,D) Change tendency of costimulatory signals and coinhibitory signals after immunotherapy. (E,F) Immunophenogram calculated according expression profiles of CDC biopsies collected at preimmunotherapy (left) and postimmunotherapy (right) time points. MHC molecules (MHC), immunomodulators (CP), ECs and SCs. CDC, collecting duct carcinoma; CP, checkpoint; EC, effector cell; MHC, major histocompatibility complex; SC, suppressor cell.

Meanwhile, we also discovered that some classical costimulatory factors showed a certain upregulation in the patient's tumor tissue after three cycles of neoantigen-based immunotherapy, such as CD70 and 4-1BB, all of which have been reported to be key regulators in the activation of T cells[21] (figure 3C). Correspondingly, as commonly reported in immunotherapy, several coinhibitory immune checkpoint molecules also showed a certain upregulation, such as IDO1 and LAG3 (figure 3D), suggesting a negative feedback regulation of T-cell activation. Furthermore, we also obtained the immunophenoscore diagrams of the tumor before and

after immunotherapy to show the immune landscape changes.[22] However, no obvious differences were observed (figure 3E,F and online supplementary figure S1B).

In summary, our results provide the first evidence to support the feasibility of personalized neoantigen-based immunotherapy for treating CDC with low mutational burden.

DISCUSSION AND CONCLUSION

The neoantigen burden in tumor tissue is directly and positively correlated with tumor mutation loads. Recently, the

neoantigen burden has been reported to be significantly associated with the clinical outcomes of immunotherapy and patient's prognosis. For those cancers with high mutation loads (also possibly high neoantigen burden), such as melanoma or lung cancer, immune checkpoint blockade therapy and neoantigen-based immunotherapy have been demonstrated to have robust clinical responses.[10 13] However, it remains unclear whether cancers with low mutation loads (possibly low neoantigen burden) could respond to neoantigen-based immunotherapy. Previous studies have reported robust immune responses triggered by neoantigen vaccine for facilitating tumor rejection in certain types of cancer with low mutation loads and neoantigen burden, including glioblastoma[9]; this study has opened a new window for treating end-stage cancers with low neoantigen burden through neoantigen-based immunotherapy strategies. CDC is a rare renal cell carcinoma (RCC) with low level of mutation loads among solid tumors,[23] and there are no good therapeutic choices for the patients with end-stage CDC. Consistently in our study, we have identified only 21 nonsynonymous somatic mutations with VAF>0.1, and 13 of them were predicted neoantigens for the enrolled patients with CDC. Fortunately, after receiving our personal neoantigen vaccination and NRT therapy, this patient have achieved stable disease status up to 9 months at both primary CDC tumor and metastatic lesions, although the antitumor activity of our prepared NRT cells still needs to be further confirmed by *in vitro* cultured patient-derived tumor cells, which sometimes are very difficult due to the lack of enough patient's tumor materials. Overall, the clinical outcomes suggest that patients with CDC and even patients with RCC with relatively low mutation loads and neoantigen loads might also be sensitive to neoantigen-based immunotherapy. However, tumor remission was still not achieved for this patient, and it might be due to the existence of tumor evolution for immune resistance or immune escape under the pressure of immunotherapy. Correspondingly, we have observed the decrease of variant allele frequency of identified neoantigens in post-treatment biopsy and the emergence of novel mutations and neoantigens, demonstrating the dynamic evolution behaviors of the tumor when it interacts with the immune microenvironment. Therefore, combining with other therapeutic strategies, such as checkpoint blockade (especially PD-1 (Programmed cell death protein 1) or PD-L1 (Programmed cell death-Ligand 1) antibodies) or radiotherapy, might further improve patients' clinical outcomes.

In conclusion, our study revealed that the neoantigen-based immunotherapy could be particularly beneficial for progression-free survival of patients with advanced CDC and might serve as a feasible therapeutic approach for future CDC treatment.

Author affiliations
[1]The United Innovation of Mengchao Hepatobiliary Technology Key Laboratory of Fujian Province, Mengchao Hepatobiliary Hospital of Fujian Medical University, Fuzhou 350025, China
[2]Mengchao Med-X Center, Fuzhou University, Fuzhou 350116, China
[3]Department of Respiratory and Critical Care Medicine, Changhai Hospital of The Second Military Medical University, Shanghai 200433, China
[4]Institute of Cardiovascular Development and Translational Medicine, The Second Affiliated Hospital and Yuying Children's Hospital of Wenzhou Medical University, Wenzhou 325027, China

ORCID iD
Xiaolong Liu http://orcid.org/0000-0002-3096-4981

REFERENCES

1 Van Poppel H, Lerut E, Oyen R, *et al*. Collecting Duct Carcinoma. In: Malouf GG, Tannir NM, eds. *Rare kidney tumors: comprehensive multidisciplinary management and emerging therapies*. Cham: Springer International Publishing, 2019: 77–92.
2 Seo AN, Yoon G, Ro JY. Clinicopathologic and molecular pathology of collecting duct carcinoma and related renal cell carcinomas. *Adv Anat Pathol* 2017;24:65–77.
3 Zhu L, Wang Z, Pan C, *et al*. Surgical monotherapy may be a suitable therapeutic strategy for advanced collecting (Bellini) duct carcinoma: a case report and literature review. *Exp Ther Med* 2016;12:1181–4.
4 Sheng X, Cao D, Yuan J, *et al*. Sorafenib in combination with gemcitabine plus cisplatin chemotherapy in metastatic renal collecting duct carcinoma: a prospective, multicentre, single-arm, phase 2 study. *Eur J Cancer* 2018;100:1–7.
5 Sun Z, Chen F, Meng F, *et al*. Mhc class II restricted neoantigen: a promising target in tumor immunotherapy. *Cancer Lett* 2017;392:17–25.
6 Snyder A, Chan TA. Immunogenic peptide discovery in cancer genomes. *Curr Opin Genet Dev* 2015;30:7–16.
7 Parkhurst MR, Robbins PF, Tran E, *et al*. Unique neoantigens arise from somatic mutations in patients with gastrointestinal cancers. *Cancer Discov* 2019;9:1022–35.
8 Yang W, Lee K-W, Srivastava RM, *et al*. Immunogenic neoantigens derived from gene fusions stimulate T cell responses. *Nat Med* 2019;25:767–75.
9 Keskin DB, Anandappa AJ, Sun J, *et al*. Neoantigen vaccine generates intratumoral T cell responses in phase Ib glioblastoma trial. *Nature* 2019;565:234–9.

10 Rosenthal R, Cadieux EL, Salgado R, *et al*. Neoantigen-directed immune escape in lung cancer evolution. *Nature* 2019;567:479–85.

11 Li H, Durbin R. Fast and accurate short read alignment with Burrows-Wheeler transform. *Bioinformatics* 2009;25:1754–60.

12 Cibulskis K, Lawrence MS, Carter SL, *et al*. Sensitive detection of somatic point mutations in impure and heterogeneous cancer samples. *Nat Biotechnol* 2013;31:213–9.

13 Dobin A, Davis CA, Schlesinger F, *et al*. Star: ultrafast universal RNA-seq aligner. *Bioinformatics* 2013;29:15–21.

14 Gerstung M, Papaemmanuil E, Campbell PJ. Subclonal variant calling with multiple samples and prior knowledge. *Bioinformatics* 2014;30:1198–204.

15 McLaren W, Gil L, Hunt SE, *et al*. The Ensembl variant effect predictor. *Genome Biol* 2016;17:122.

16 Jurtz V, Paul S, Andreatta M, *et al*. NetMHCpan-4.0: improved peptide-MHC class I interaction predictions integrating eluted ligand and peptide binding affinity data. *J Immunol* 2017;199:3360–8.

17 Andreatta M, Karosiene E, Rasmussen M, *et al*. Accurate pan-specific prediction of peptide-MHC class II binding affinity with improved binding core identification. *Immunogenetics* 2015;67:641–50.

18 Miller CA, White BS, Dees ND, *et al*. SciClone: inferring clonal architecture and tracking the spatial and temporal patterns of tumor evolution. *PLoS Comput Biol* 2014;10:e1003665.

19 Szolek A, Schubert B, Mohr C, *et al*. OptiType: precision HLA typing from next-generation sequencing data. *Bioinformatics* 2014;30:3310–6.

20 Boegel S, Löwer M, Schäfer M, *et al*. Hla typing from RNA-seq sequence reads. *Genome Med* 2012;4:102.

21 Driessens G, Kline J, Gajewski TF. Costimulatory and coinhibitory receptors in anti-tumor immunity. *Immunol Rev* 2009;229:126–44.

22 Charoentong P, Finotello F, Angelova M, *et al*. Pan-Cancer Immunogenomic analyses reveal Genotype-Immunophenotype relationships and predictors of response to checkpoint blockade. *Cell Rep* 2017;18:248–62.

23 Matsushita H, Sato Y, Karasaki T, *et al*. Neoantigen load, antigen presentation machinery, and immune signatures determine prognosis in clear cell renal cell carcinoma. *Cancer Immunol Res* 2016;4:463–71.